International Journal for Housing Science and Its Applications
Publish August 10, 2025. Volume 46, Issue 4 Pages 5978-5990

https://doi.org/10.70517/ijhsa464435

GIS Equipment Status Assessment Method for Substations Based on Multi-Frequency Signal Processing

Jinjin Xu[1,*]
[1] School of Electronics & Computer Science, University of Southampton, Southampton, Hampshire, SO17 1BJ, UK
Corresponding authors: (e-mail: jx1n2024@163.com).

Abstract Traditional state assessment methods often rely on single frequency signals and can only detect faults within a specific frequency range, making it difficult to fully reflect the overall state of the equipment. This article introduces multi-frequency signal processing technology to evaluate the status of GIS (Geographic Information System) equipment in substations. Firstly, the signal's global spectrum features are extracted using the Fourier transform, and its properties at various time and frequency scales are obtained by time-frequency analysis using the wavelet transform. Then, spectral and time-frequency feature parameters are extracted from the decomposed signal, and decision level fusion using voting method is used to fuse the signal features of different frequencies and types, and output a comprehensive feature vector. Finally, the LSTM (Long Short-Term Memory) algorithm is used to analyze the fused feature vectors and evaluate the status of GIS equipment. The experiment was based on the log data of a substation company in Wuhan from June to December 2023, and combined with multi-frequency signal processing to evaluate the status of GIS equipment. The results showed that the accuracy of state evaluation by integrating multi-frequency signal processing and LSTM method reached 98.25%. Compared to the accuracy based on a specific frequency range, it has improved by 8.53%, and the shortest response time is only 1.8s. Experiments have shown that multi-frequency signal processing plays an important role in the comprehensive evaluation of GIS equipment status in substations, greatly improving the accuracy of evaluation, achieving accurate reflection of the overall status of GIS equipment, and promoting the stable operation of substations.

Index Terms Multi-frequency Signal Processing, State Evaluation, GIS Equipment, LSTM Algorithm, Fault Detection

I. Introduction

Substation GIS equipment is a key component of the power system, and its operating status directly affects the power supply. Previous single-frequency signal detection can only detect faults within a specific frequency range and cannot show the overall situation [1]. These studies are often limited by the frequency range, resulting in incomplete signal feature extraction and insufficient fault detection accuracy [2]. As the power system becomes more and more complex, the status assessment of substation GIS equipment has become more difficult. To solve this problem, people have begun to explore more advanced multi-frequency signal processing technology.

This article adopts an innovative multi-frequency signal processing method for substation GIS equipment status assessment. This method improves the comprehensive monitoring capability of equipment status through multi-frequency signal feature extraction and fusion technology. It improves the sensitivity and stability of fault detection, optimizes the accuracy of status assessment, enhances the effect of signal processing, and provides a new technical means for status monitoring and fault prevention of substation GIS equipment.

II. Related Work

Researchers use different technical methods to evaluate the status of GIS equipment in substations. YU Cong et al. introduced the partial discharge signal fusion decision based on time-resolved partial discharge and phase resolved partial discharge into the proposed BP (Back Propagation) neural network and improved DS (Dempster-Shafer) evidence theory diagnostic method, and performed fault identification by introducing evidence fusion degree [3]. Qingcheng Lin et al. designed a simplified model to approximately describe the internal insulation structure of GIS [4]. Shunfan He et al. proposed an electrical feature detection and analysis method for monitoring various power equipment faults in intelligent substations [5]. Xi Li et al. reviewed a large amount of research on local discharge source localization and proposed location of a local discharge source method founded on Support Vector Machine (SVM) and picture edge detection [6]. Yan-Bo Wang et al. introduced a universal

separation method based on Linear Predictive Analysis (LPA) and Isolation Forest (IF) algorithm [7]. There are also studies using the hybrid AHP-TOPSIS(Analytic Hierarchy Process - Technique for Order of Preference by Similarity to Ideal Solution) method to provide a decision support framework for substation technology selection [8]. D'Souza M et al. introduced the modern concept and methods of modularity, describing the technological development, design philosophy, quality assurance, and environmental impact of providing complete solutions based on site conditions [9]. Hongzhong Ma et al. implemented a non-invasive method that took vibration signals triggered by circuit breaker action into account while assessing the mechanical state of GIS [10]. Ren M et al. introduced an ultra-sensitive three-band optical PD sensor and obtained the spectral information by this new optical sensor [11]. Yanxin Wang and Xiaosheng Peng et al. attempted to combine convolutional neural networks to classify extracted signal features and improve the accuracy of fault detection [12], [13]. Khalyasmaa A I et al. used decision tree-based machine learning to address the possibility of evaluating the technical status of power circuit breakers, and solved the problem of determining their optimal parameters and training samples [14]. Janani H et al. proposed a defect feature extraction and classification algorithm for high-voltage gas insulation systems based on the statistical analysis of partial discharge (PD) signal time domain parameters, focusing on measuring and interpreting PD signals in the time domain [15]. Hamed Janani et al. proposed a new algorithm for the analysis and separation of PD pulse waveforms based on the Laguerre polynomial orthogonal series expansion, and also developed a system identification technology to help improve the accuracy of signal classification [16]. Xinlu Yang et al. used RBF (Radial Basis Function) neural network to classify defects. Through experiments, the high recognition rate was verified, indicating the effectiveness and applicability of the proposed method [17]. Salkuti S R introduced the differences between SCADA (Supervisory Control And Data Acquisition) and substation automation, as well as the concept of substation automation. The reliability assessment of smart grids can be carried out through analysis or simulation. The analysis method utilizes load point evaluation techniques, while the simulation technique uses Monte Carlo simulation techniques. The reliability index evaluation can consider the presence of energy storage components [18]. However, there are still shortcomings in the comprehensiveness of signal feature extraction and the sensitivity of fault detection in current research, and more comprehensive methods are urgently needed to solve these problems.

To address the issues in current research, some researchers have adopted different methods for improvement. Banihashemi S et al. introduced an algorithm for planning green spaces aimed at optimizing the location, size, and power supply area of medium and low voltage substations in the Reference Network Model (RNM) [19]. Shudong Wang et al. proposed a multi-resolution generalized S-transform (GST) denoising algorithm for precise localization of partial discharge in substations, achieving accurate localization of partial discharge [20]. There is also research on using SVM to achieve casing fault diagnosis [21]. Another part of the research has shown good results in power outage prediction and fault detection using deep learning algorithms [22], [23]. Bhukya A et al. achieved better performance by combining the Bi-LSTM (Bi-directional Long Short-Term Memory) model with an enhanced training set [24]. Xue J et al. effectively simulated the situation of power grid equipment by combining the dynamic analysis of equipment in GIS and deep learning of nonlinear network structures [25]. Dukanac D et al. proposed a new program for extracting PD signals in the main high-frequency range from the strong noise of each signal in power transformers [26]. Tian D et al. proposed an improved YOLOv4 algorithm based on a hybrid domain attention mechanism for designing an intelligent substation inspection system [27]. There are also studies that use self-learning methods to achieve online monitoring after fiber optic cable faults occur [28]. However, these methods still have room for improvement in feature fusion and temporal modeling. This article introduces multi-frequency signal processing technology, combined with LSTM algorithm, to comprehensively evaluate the status of GIS equipment in substations, aiming to improve the accuracy and reliability of the evaluation.

III. Implementation Based on Multi-Frequency Signal Processing

III. A. Global Spectrum Feature Extraction

In the assessment of GIS equipment status in substations, the frequency domain characteristics of signals can reflect the operating status and potential fault information of the equipment [29]. To extract global spectral features, Fourier Transform is used to transform the time-domain signal. Fourier transform decomposes the time signal into harmonic components of different frequencies, thereby obtaining the global spectrum characteristics.

The collected operating signal data of the substation GIS equipment comes from the log records of a substation company in Wuhan from June to December 2023. These time domain signals are preprocessed to remove noise and interference. The processed signal data is input into the Fourier transform algorithm for frequency domain conversion. The core formula of Fourier transform is:

$$X(f) = \int_{-\infty}^{\infty} x(t) e^{-j2\pi f} \, dt \tag{1}$$

$X(f)$ represents frequency domain signal, $x(t)$ represents time domain signal, f represents frequency, t and j respectively refer to time and imaginary units.

After Fourier transformation, the time domain signal is converted into a frequency domain signal, and then the spectrum characteristics of the signal are obtained from the frequency domain signal. The spectrum diagram is used to visualize and display the spectrum characteristics more intuitively. The diagram can show the signal's amplitude variations at every frequency component.

Figure 1 shows the detailed process from collecting time domain signal data to analyzing spectrum features. This process makes the signal feature extraction comprehensive.

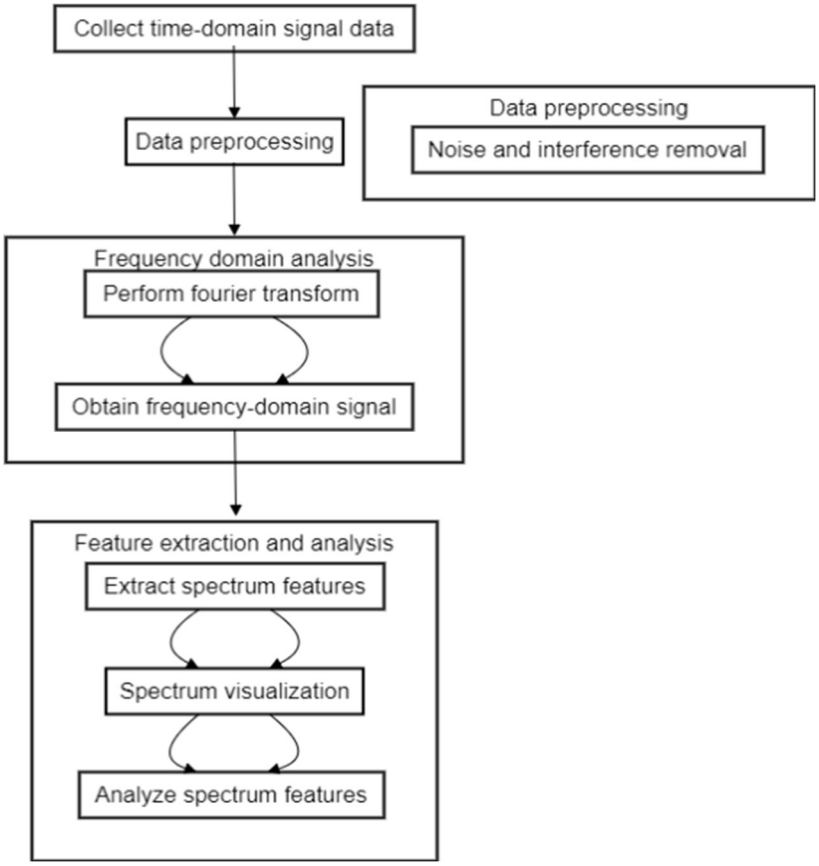

Figure 1: Spectral Feature Extraction Process Based on Fourier Transform

Table 1 is the spectrum characteristic data obtained after processing:

Table 1: Raw Signal and Spectral Feature Data

Sample Time (s)	Signal Amplitude (mV)	Frequency (Hz)	Amplitude Spectrum (dB)
0	1.2	50	-20
0.1	1.5	100	-15
0.2	1.1	150	-25
0.3	1.3	200	-10
0.4	1.4	250	-18

The extracted spectrum feature data shows the amplitude changes of the signal. These changes reflect the energy distribution of the equipment at different frequencies and reveal the operating characteristics of GIS equipment at different frequencies.

III. B. Time Frequency Analysis

The signal is subjected to time-frequency analysis using the wavelet transform. Wavelet transform analyzes the signal in two dimensions: time and frequency, and extracts the signals' local characteristics [30].

After preprocessing, the time-frequency characteristics of the signal are obtained by applying the wavelet transform to the time domain signal. The formula is:

$$W_\psi(a,b) = \int_{-\infty}^{\infty} x(t)\psi^*(\frac{t-b}{a})dt \quad (2)$$

$W_\psi(a,b)$ is the wavelet coefficient of signal $x(t)$ at scale a and translation b, $\psi(t)$ is the mother wavelet, and $*$ represents complex conjugation.

To confirm the competence of wavelet transform in capturing the instantaneous and local characteristics of the signal, the signal is processed by wavelet transform in normal state and fault state respectively. Table 2 shows the wavelet coefficient data in normal state and fault state.

Table 2: Signal and wavelet coefficient data under normal and fault conditions

Sample Time (s)	Signal Amplitude (Normal)	Scale (a)	Wavelet Coefficient (Normal)	Signal Amplitude (Fault)	Wavelet Coefficient (Fault)
0	1.8	1	0.42	2.2	0.65
0.1	1.9	2	0.47	2.3	0.72
0.2	2	3	0.33	2.1	0.58
0.3	2.1	4	0.41	2.5	0.63
0.4	1.7	5	0.52	2.4	0.75

After analyzing the data in the table, it is found that the use of wavelet transform does capture the instantaneous and the signal's local properties. By comparing the frequency-time characteristics under normal and fault conditions, the abnormal conditions in the operation of the equipment can be accurately identified. The results show that wavelet transform has obvious effects in signal feature extraction and fault detection.

Figure 2 shows the energy distribution of the signal in time and frequency in normal and faulty states. It is not difficult to see from the figure that the signal's energy in its usual state is mainly concentrated in the lower frequency range, and the amplitude is relatively stable. In the faulty state, the energy of the signal in the higher frequency range is obviously increased, and the energy distribution is more dispersed, and the amplitude is also higher. The obvious difference in frequency and time energy shows the effect of wavelet transform in this field.

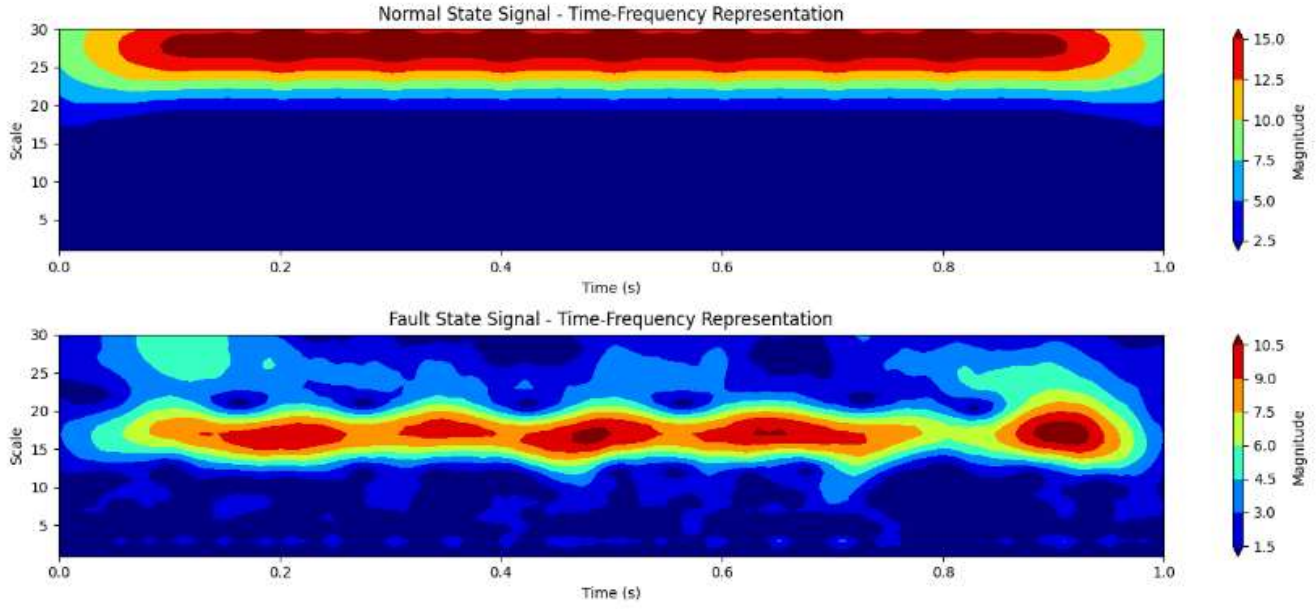

Figure 2: Signal time-frequency diagram under different states

III. C. Signal Decomposition

Discrete Wavelet Transform (DWT) is used to perform multi-scale decomposition of the signal to extract signal feature parameters of different frequencies and types. DWT decomposes the signal into sub-bands of different scales, which helps to extract the multi-scale features of the signal [31].

The preprocessed signal data is input into the DWT algorithm for multi-scale decomposition. The calculation formula for DWT is as follows:

$$X_j(t) = \sum_{k=-\infty}^{\infty} x(k)\psi(2^{-j}t - k) \tag{3}$$

$$A_j(t) = \sum_{k=-\infty}^{\infty} x(k)\phi(2^{-j}t - k) \tag{4}$$

$X_j(t)$ and $A_j(t)$ respectively represent detail coefficients and approximation coefficients, $\psi(t)$ is a wavelet function, $\phi(t)$ is a scale function, j and k are scale and displacement, respectively.

After applying DWT, the signal is decomposed into several sub bands of different scales, each containing detailed information about the signal at different frequencies. Features of the multi-scale signal can be extracted from these sub-band data. Table 3 displays the experiment's initial data as well as the signal feature data following multi-scale decomposition:

Table 3: Signal feature data after DWT decomposition

Sample Time (s)	Signal Amplitude (mV)	Scale (a)	Detail Coefficient	Approximate Coefficient
0	1.1	1	0.25	0.45
0.1	1.3	2	0.35	0.5
0.2	1.2	3	0.4	0.55
0.3	1.4	4	0.45	0.6
0.4	1.5	5	0.5	0.65

The data in Table 3 shows the detail coefficients and approximation coefficients at different sample times and scales. The sample time is 0.0 seconds, the detail coefficient of scale 1 is 0.25, and the approximation coefficient is 0.45. By comparing data at different times and scales, it can find out how the signal changes in different frequency components. In summary, DWT can effectively decompose signals and extract multi-scale features. Multi-scale features reflect the detailed information of the signal at each frequency component so as to understand the operating status of the equipment. Using these features, the evaluation model can more accurately identify normal and abnormal conditions.

The excellent performance of DWT in signal decomposition increases the credibility of the status assessment results of substation GIS equipment. The details and approximate coefficients calculated by DWT show the properties of the signal over various scales.

III. D. Feature Fusion

In terms of signal feature fusion, the voting method is used for decision-level fusion, and signal features of different frequencies and types are weightedly combined to generate a comprehensive feature vector.

During the feature fusion process, the extracted signal features are normalized to make the different features have consistent dimensions. The weight matrix is then defined based on the contribution of each feature to the evaluation result, and the optimal configuration is determined through the optimization of experimental data.

The setting of weights requires multiple experiments to adjust the weight values of each feature, ensuring that the comprehensive feature vector can accurately reflect the state of the device. The application formula of the weight matrix is:

$$F_{fusion} = \sum_{i=1}^{n} w_i F_i \tag{5}$$

Among them, the comprehensive feature vector is represented by F_{fusion}, w_i is the weight of the ith feature, and F_i is the ith feature.

In practical operation, all extracted features are preprocessed to ensure the quality of the data. Suitable weight matrices can be selected for weighted calculation, and the selection and optimization of weight matrices are carried out through cross validation until the optimal configuration is found. Each feature is assigned different weights during the fusion process based on its contribution to the evaluation results. In the experiment, the weight allocation of different feature types is shown in the data distribution in Table 4:

Table 4: Weight distribution of feature fusion

Feature Type	Weight	Frequency (Hz)	Time-Frequency Feature (dB)
Spectrum Feature 1	0.2	50	-20
Spectrum Feature 2	0.3	100	-15
Time-Frequency Feature 1	0.25	150	-25
Time-Frequency Feature 2	0.25	200	-10

The weight allocation of different feature types shows their contribution in the comprehensive feature vector. The optimal weight matrix configuration can be determined through continuous adjustment and optimization of experimental data. The integrated feature vector after fusion more accurately reflects the status of GIS equipment in substations.

The following Table 5 is an example of data for adjusting different feature weights during the experimental process:

Table 5: Evaluation indicators during weight adjustment process

Iteration	Spectrum Feature 1 Weight	Spectrum Feature 2 Weight	Time-Frequency Feature 1 Weight	Time-Frequency Feature 2 Weight	Accuracy (%)	Fault Detection Rate (%)	False Alarm Rate (%)
1	0.25	0.25	0.25	0.25	92.1	88.4	5.6
2	0.2	0.3	0.25	0.25	93.5	89.2	4.8
3	0.15	0.35	0.25	0.25	94.2	90.1	4.2
4	0.1	0.4	0.25	0.25	94.8	91	3.9

From the data in Table 5, it can be seen that by gradually adjusting the feature weights, the evaluation accuracy and fault detection rate continue to improve, while the false alarm rate gradually decreases. The final optimal weight configuration is: Spectrum Feature 1 has a weight of 0.1, Spectrum Feature 2 has a weight of 0.4, Time Frequency Feature 1 has a weight of 0.25, and Time Frequency Feature 2 has a weight of 0.25. Under this configuration, the evaluation accuracy reached 94.8%, the fault detection rate was 91.0%, and the false alarm rate was reduced to 3.9%.

Through continuous adjustment and optimization of experimental data, the optimal weight matrix configuration was ultimately determined, significantly improving the performance of the evaluation model. The experimental data verified that the decision-level fusion method of voting method is feasible in GIS equipment status assessment.

III. E. Status Assessment

When analyzing the feature vector after feature fusion, the long short-term memory network (LSTM) algorithm is used for state evaluation. LSTM is a special recursive neural network (RNN). The structure of LSTM is divided into input gate, forget gate, output gate and memory cell. Each gate control unit realizes dynamic processing of signals and extraction of time series features by controlling the flow of information.

The following is the LSTM computation methodology:

$$f_t = \sigma(W_f \cdot [h_{t-1}, x_t] + b_f) \tag{6}$$

$$i_t = \sigma(W_i \cdot [h_{t-1}, x_t] + b_i) \tag{7}$$

$$\tilde{C}_t = \tanh(W_C \cdot [h_{t-1}, x_t] + b_C) \tag{8}$$

$$C_t = f_t * C_{t-1} + i_t * \tilde{C}_t \tag{9}$$

$$o_t = \sigma(W_o \cdot [h_{t-1}, x_t] + b_o) \tag{10}$$

$$h_t = o_t * \tanh(C_t) \tag{11}$$

σ represents the Sigmoid function, W is the weight matrix, b is the bias, x_t refers to the current input, h_{t-1} is the hidden state at the previous time, and C_t is the current memory cell state.

The experimental data contains multiple time series signals, which are supplied as training data to the LSTM model and evaluation after feature extraction and fusion. Table 6 shows the evaluation results in the experiment.

Table 6: Raw Signal Data and LSTM Prediction Results

Sample Time (s)	Signal Amplitude (mV)	LSTM Prediction	Actual State
0	1.1	Normal	Normal
0.1	1.2	Normal	Normal
0.2	0.8	Fault	Fault
0.3	1.3	Normal	Normal
0.4	0.7	Fault	Fault

As observed in the table, the LSTM model's prediction results are highly similar to the actual status, indicating that it is also effective in capturing signal timing characteristics and evaluating the status of GIS equipment. Testing on multiple samples verifies the positive performance of the LSTM model.

The prediction findings demonstrate that the LSTM model's ability to precisely assess the status of substation GIS equipment by analyzing the fused feature vectors when processing complex time series data.

IV. Evaluation Results and Analysis

IV. A. Accuracy of State Assessment

In order to evaluate the performance of the fusion of multi-frequency signal processing and LSTM method in the condition assessment of substation GIS equipment, the condition assessment accuracy is used as the key indicator of the experiment. During the evaluation process, multiple and comparative experiments are used to evaluate the performance of the model under different experimental conditions.

The experiment used log record data from a substation company in Wuhan from June to December 2023. After processing, these data were input into the LSTM model for training and testing. The model evaluates the status of GIS equipment by learning the temporal relationship inside the data time series.

The accuracy of state assessment is calculated by comparing the level of correspondence between the model's anticipated and real states. The definition of accuracy is the ratio of the number of correctly predicted samples to the total number of samples, and the calculation equation is as follows:

$$\text{Accuracy} = \frac{\text{NumberofCorrectPredictions}}{\text{TotalNumberofPredictions}} \times 100\% \tag{12}$$

The test set included 10,000 samples during the experiment, and 9825 of those samples had their states properly predicted by the LSTM model. The accuracy of the evaluation was calculated to be 98.25%. The single frequency signal analysis method correctly predicted 8972 samples, with an accuracy of only 89.72%, which is an improvement of 8.53% compared to the previous method.

Table 7 shows some of the experimental data and results:

Table 7: Raw Signal Data and LSTM Prediction Results

Sample Time (s)	Signal Amplitude (mV)	Predicted State	Actual State
0	1.1	Normal	Normal
0.1	1.2	Normal	Normal
0.2	0.8	Fault	Fault
0.3	1.3	Normal	Normal
0.4	0.7	Fault	Fault
0.5	1.5	Normal	Normal
0.6	0.9	Fault	Fault
0.7	1.4	Normal	Normal
0.8	1	Normal	Normal
0.9	0.6	Fault	Fault

From the experimental data in Table 7, it can be concluded that the LSTM model's predicted state of signal amplitude at different time points is highly consistent with the actual state, demonstrating the high accuracy of the model in state evaluation. However, to confirm the model's dependability and stability, multiple experiments and cross validation were conducted on the model.

By evaluating the performance of the model under different experimental conditions, the findings of the experiment indicate that the feature extraction method and model parameters have a significant impact on the accuracy of the evaluation. The evaluation accuracy of the LSTM model under different experimental conditions is

shown in Figure 3. The results show that the evaluation accuracy can reach up to 98.25% using the optimized feature extraction method and LSTM model parameters. This high accuracy shows the feasibility of integrating multi-frequency signal processing and LSTM method in substation GIS equipment status evaluation.

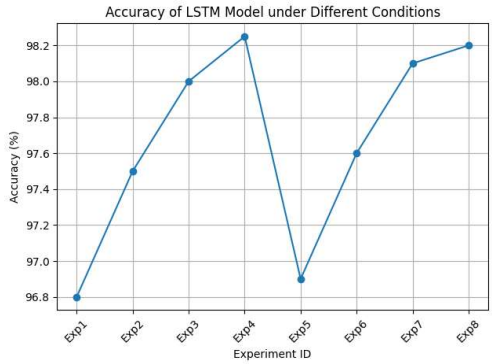

Figure 3: Accuracy of LSTM model under different conditions

IV. B. Response Time

Response time is a key indicator that measures the efficiency of the system in processing and evaluation. To verify the performance of the LSTM model in response time, a control experimental model was used for validation. Each experiment was conducted using four models, LSTM, SVM, RF, and NN (Neural Network), to prevent the occurrence of randomness. In the experiment, the data is preprocessed to remove noise and interference, ensuring the purity and effectiveness of the signal. In terms of feature extraction, the global spectrum properties of the signal are extracted using the Fourier transform, and the wavelet transform is employed to obtain the features of the signal at different time and frequency scales. Feature fusion adopts decision level fusion using voting method, which weights and combines signal features of different frequencies and types to generate a comprehensive feature vector.

The experimental data still comes from the log records of a substation company in Wuhan, which record the operation of the substation GIS equipment at different time points. The calculation of response time is achieved by recording the time from signal input to model output evaluation results each time. Figure 4 shows the response time of different models in the experiment, and four subgraphs respectively demonstrate the performance of LSTM, SVM, RF, and NN models. The LSTM model performed well in all experiments, with the shortest response time ranging from 1.80 seconds to 1.82 seconds. The response time of other models is significantly longer, with SVM ranging from 2.45 seconds to 2.60 seconds, RF ranging from 2.18 seconds to 2.30 seconds, and NN ranging from 1.95 seconds to 2.05 seconds. This indicates that the LSTM model has the highest efficiency and significant advantages in processing the status assessment of GIS equipment in substations.

The evaluation results of response time show that the LSTM model is an ideal choice for substation GIS equipment status evaluation.

IV. C. Fault Detection Rate

Fault detection rate is the ability of the evaluation system to detect equipment failures. Fault detection is crucial for the operation and maintenance of substation GIS equipment. As a key component of the power system, the normal operation of substation GIS equipment directly affects the safety of the power grid.

The calculation of fault detection rate is expressed as:

$$\text{Fault Detection Rate} = \frac{\text{Number of Detected Faults}}{\text{Total Number of Faults}} \times 100\% \tag{13}$$

Table 8 shows the number of faults detected in the experiment and the total number of faults:

Table 8: Comparison of Fault Detection between Single Frequency and Multi-Frequency Methods

Experiment ID	Total Faults	Detected Faults (Single Frequency)	Detection Rate (Single Frequency) (%)	Detected Faults (Multi-Frequency)	Detection Rate (Multi-Frequency) (%)
Exp1	100	85	85	96	96
Exp2	100	83	83	95	95
Exp3	100	84	84	94	94
Exp4	100	86	86	97	97
Exp5	100	85	85	96	96

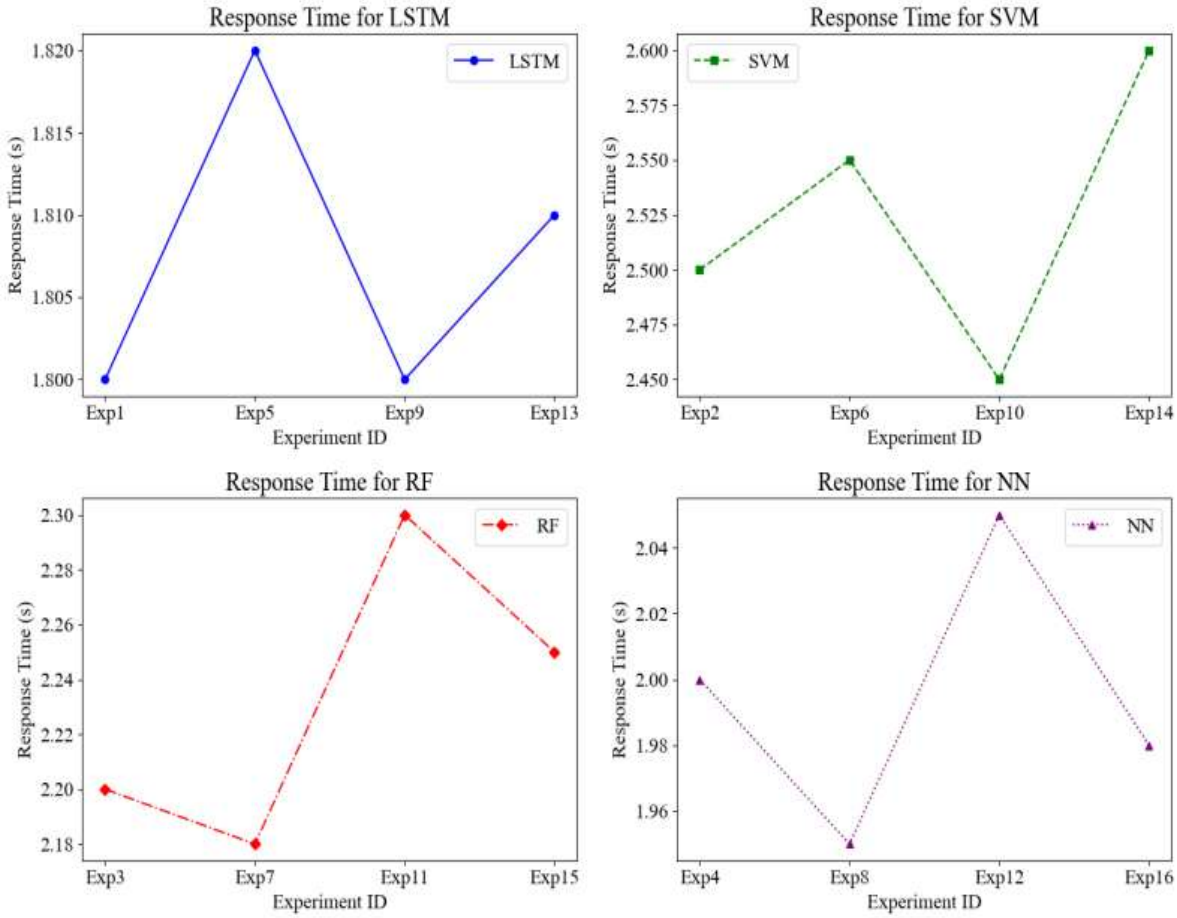

Figure 4: Comparison of response times of different models

The findings indicated that the rate of fault detection of the single-frequency signal analysis method ranged from 83% to 86%, with an average fault detection rate of 84.6%. The fault detection rate of the fusion multi-frequency signal processing and LSTM method is between 94% and 97%, and the average fault detection rate is 95.6%. Comparing the single frequency signal analysis method with the fusion multi-frequency signal processing method, it is found that the fusion multi-frequency signal processing and LSTM method performs well in fault detection.

However, to confirm the method's efficacy even more, this article contrasts the fault detection rates using support vector machines (SVM), random forests (RF), and traditional neural networks (NN), as displayed in Figure 5. The fault detection rate of the LSTM model in all experimental groups remained at 94%-97%, and was the highest value in each group. This also shows that the LSTM model performs best in fault detection, and the fault detection effect of the fusion of multi-frequency signal processing and LSTM method is the most accurate.

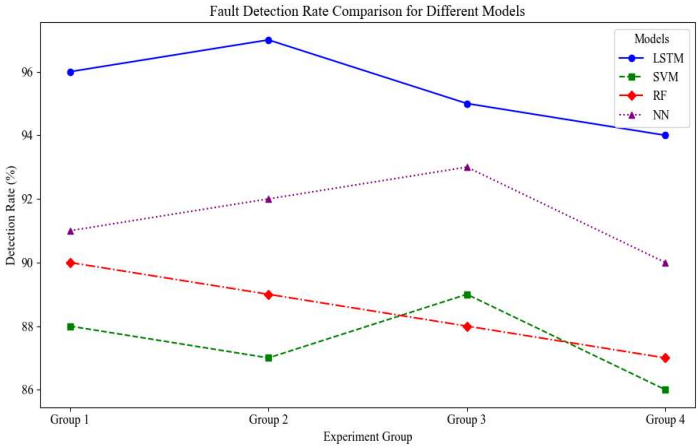

Figure 5: Comparison of fault detection rates of various experimental groups

The comparative experiments and the fault detection comparison between single-frequency and multi-frequency methods have verified the advantages of the fusion of multi-frequency signal processing and LSTM methods in fault detection. A higher fault detection rate means that equipment faults can be discovered and handled more promptly, reducing downtime and ensuring the stable operation of the substation.

IV. D. False Alarm Rate

The false alarm rate is the frequency of errors in the fault detection process of the evaluation system. A lower false alarm rate can improve the credibility of the method in practical application, allowing operation and maintenance personnel to trust the evaluation results more and make more accurate maintenance decisions.

The calculation formula for the false alarm rate is as follows:

$$\text{False Alarm Rate} = \frac{\text{Number of False Alarms}}{\text{Total Number of Evaluations}} \times 100\% \tag{14}$$

Table 9 shows five sets of experimental results for false alarm rate detection.

Table 9: Experimental statistical result

Experiment ID	Total Evaluations	False Alarms	False Alarm Rate (%)
Exp1	100	3	3
Exp2	100	4	4
Exp3	100	2	2
Exp4	100	3	3
Exp5	100	3	3

From the data in the table, it can be concluded that the false alarm rate of the fusion multi-frequency signal processing and LSTM method is stable at 2%-4%, as well as the result's average false alarm rate is 3.00%. The low number of false alarms indicates that the technique has a low number of false positives in practical applications.

However, in order to prevent errors, four groups of comparative experiments were conducted for more convincing verification. The comparative experiments also used support vector machine (SVM), random forest (RF) and traditional neural network (NN) as controls. The four sub-figures in Figure 6 show the comparison of the false alarm rate of the models in different experimental groups. The statistical results show that the LSTM model has the lowest false alarm rate in the four experimental groups. The false alarm rates of the other three methods are higher than that. The emergence of this result further shows that the fusion of multi-frequency signal processing and LSTM method can significantly reduce the false alarm rate.

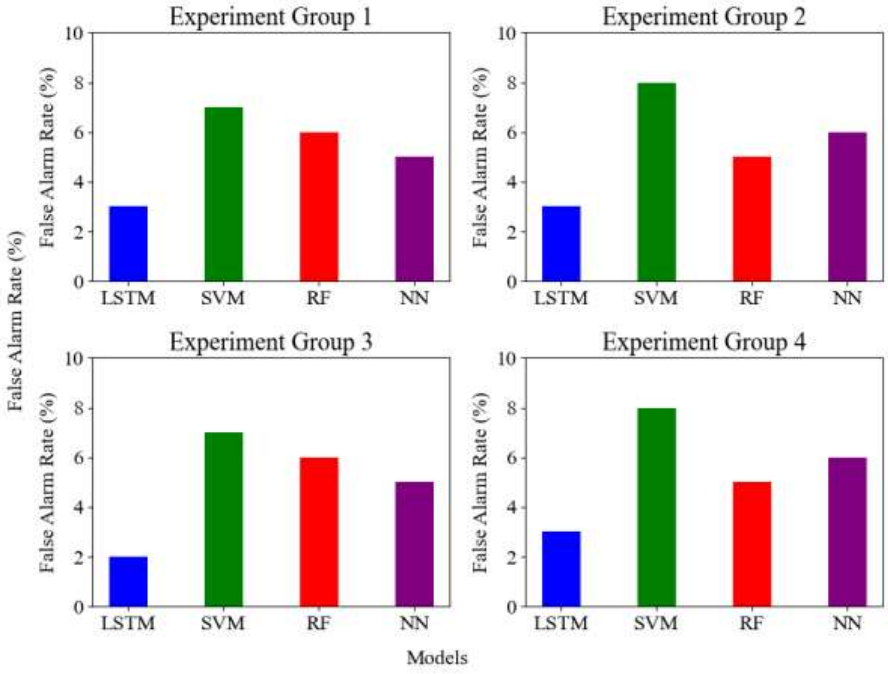

Figure 6: Comparison of false alarm rates of different models

Combining the results of the two experiments, it is concluded that the fusion of multi-frequency signal processing and LSTM methods performs better in terms of false alarm rate. A lower false alarm rate means that the equipment status can be assessed more accurately and misjudgment can be reduced. This is of great significance for the maintenance and management of power systems, and can help power engineers discover and deal with potential problems in a timely manner.

IV. E. Comparative Analysis

Experimental results show that multi-frequency signal processing and LSTM methods perform well on multiple key indicators, surpassing single-frequency signal analysis methods. The accuracy of state assessment has been significantly improved. The accuracy of using multi-frequency signal processing and LSTM method reaches 98.25%, which is 8.53% higher than the single-frequency signal analysis method. This shows that multi-frequency signal processing methods can capture more comprehensive signal characteristics.

In terms of response time, multi-frequency signal processing and LSTM methods show significant advantages. Experimental data shows that the response time of the multi-frequency signal processing method is only 1.8 seconds, while the response time of the single-frequency signal analysis method is longer. For real-time monitoring and fault handling of substation GIS equipment, this advantage can detect and handle equipment faults in a more timely manner and reduce downtime.

Regarding the rate of fault detection, multi-frequency signal processing and LSTM methods performed well. Experimental results show that the fault detection rate of the multi-frequency signal processing method is between 94% and 97%, while the fault detection rate of the single-frequency signal analysis method is between 83% and 86%. The multi-frequency signal processing method is significantly better than the single-frequency signal analysis method in fault detection.

The experimental results of false alarm rate show that multi-frequency signal processing and LSTM methods also show obvious advantages. The experimental results show that the false alarm rate of multi-frequency signal processing method is between 2% and 4%, with an average of 3.00%, while the false alarm rates of other models are all higher. The LSTM model performs best in terms of false alarm rate, which is much lower than other models, showing higher evaluation accuracy.

Based on the experimental results, multi-frequency signal processing and LSTM methods are superior to single-frequency signal analysis methods in terms of status assessment accuracy, response time, fault detection rate, and false alarm rate. Multi-frequency signal processing technology can capture more comprehensive signal features, and combined with the timing analysis capability of LSTM, it can achieve efficient evaluation of GIS equipment status.

By introducing more signal processing technologies and optimization algorithms, the performance of the evaluation system can be further improved, providing a stronger guarantee for the safe operation of the power system. Through continuous technical improvements and practical applications, multi-frequency signal processing and LSTM methods are expected to be promoted and applied in more fields and play a greater role.

V. Conclusions

This article introduces a comprehensive method based on multi-frequency signal processing and LSTM algorithm to evaluate the status of substation GIS equipment. In the study, Fourier transform and wavelet transform were used to extract the spectrum and time-frequency characteristics of the signal, and generated a comprehensive feature vector through feature fusion, and then used the LSTM model for state assessment. Experimental results verify the superiority of this method in terms of accuracy and response time in state assessment, showing significant improvements compared with traditional single-frequency signal analysis methods. Although the research has achieved good results, the generalization ability of the model and the optimization of feature fusion still need to be further studied. In the future, the article can further expand the dataset, optimize feature extraction and fusion algorithms, and explore more deep learning techniques to improve the performance and adaptability of the evaluation system.

References

[1] Fan Yang, Weidong Kang, Wei Hou, Hao Gu. Research on state perception method of electrical equipment in substation[J]. Journal of Artificial Intelligence Practice, 2021, 4(2): 37-42.

[2] Shibo Lu, Hua Chai, Animesh Sahoo, B. T. Phung. Condition monitoring based on partial discharge diagnostics using machine learning methods: A comprehensive state-of-the-art review[J]. IEEE Transactions on Dielectrics and Electrical Insulation, 2020, 27(6): 1861-1888.

[3] YU Cong, TANG Kaibo, LI Zhe, LIU Zhipeng, CHEN Bo, LIU Yuanchao, FANG Yaqi, et al. GIS Equipment Fault Identification Based on BP Neural Network and Improved DS Evidence Fusion[J]. Journal of Electrical Engineering, 2024, 18(4): 361-369.

[4] Qingcheng Lin, Fuyong Lyu, Shiqi Yu, Hui Xiao, Xuefeng Li. Optimized denoising method for weak acoustic emission signal in partial discharge detection[J]. IEEE Transactions on Dielectrics and Electrical Insulation, 2022, 29(4): 1409-1416.

[5] Shunfan He, Yan Zhang, Rongbo Zhu, Wei Tian. Electric signature detection and analysis for power equipment failure monitoring in smart grid[J]. IEEE Transactions on Industrial Informatics, 2020, 17(6): 3739-3750.

[6] Xi Li, Xiaohua Wang, Aijun Yang, Mingzhe Rong. Partial discharge source localization in GIS based on image edge detection and support vector machine[J]. IEEE Transactions on Power Delivery, 2019, 34(4): 1795-1802.

[7] Yan-Bo Wang, Ding-Ge Chang, Shao-Rui Qin, Yu-Hang Fan, Hai-Bao Mu, Guan-Jun Zhang. Separating multi-source partial discharge signals using linear prediction analysis and isolation forest algorithm[J]. IEEE Transactions on Instrumentation and Measurement, 2019, 69(6): 2734-2742.

[8] Ashish Trivedi, Amit Tyagi, Ouissal Chichi, Sanjeev Kumar, Vibha Trivedi. Substation technology selection for environment efficient power distribution system in India: an integrated AHP-TOPSIS-based approach[J]. International Journal of Energy Sector Management, 2024, 18(3): 617-638.

[9] D'Souza M, Dhara R S, Bouyer R C. Modularization of high voltage gas insulated substations[J]. IEEE Transactions on Industry Applications, 2020, 56(5): 4662-4669.

[10] Hongzhong Ma, Baowen Liu, Honghua Xu, Bingbing Chen, Ping Ju, Li Zhang, Bin Qu, et al. GIS mechanical state identification and defect diagnosis technology based on self-excited vibration of assembled circuit breaker[J]. IET Science, Measurement & Technology, 2020, 14(1): 56-63.

[11] Ren M, Zhou J, Miao J. Adopting spectral analysis in partial discharge fault diagnosis of GIS with a micro built-in optical sensor[J]. IEEE Transactions on Power Delivery, 2020, 36(2): 1237-1240.

[12] Yanxin Wang, Jing Yan, Zhou Yang, Yiming Zhao, Tingliang Liu. GIS partial discharge pattern recognition via lightweight convolutional neural network in the ubiquitous power internet of things context[J]. IET Science, Measurement & Technology, 2020, 14(8): 864-871.

[13] Xiaosheng Peng, Fan Yang, Ganjun Wang, Yijiang Wu, Lee Li, Zhaohui Li, et al. A convolutional neural network-based deep learning methodology for recognition of partial discharge patterns from high-voltage cables[J]. IEEE Transactions on Power Delivery, 2019, 34(4): 1460-1469.

[14] Khalyasmaa A I, Senyuk M D, Eroshenko S A. High-voltage circuit breakers technical state patterns recognition based on machine learning methods[J]. IEEE Transactions on Power Delivery, 2019, 34(4): 1747-1756.

[15] Janani H, Shahabi S, Kordi B. Separation and classification of concurrent partial discharge signals using statistical-based feature analysis[J]. IEEE Transactions on Dielectrics and Electrical Insulation, 2020, 27(6): 1933-1941.

[16] Hamed Janani, Pramoda Jayasinghe, Mohammad Jafari Jozani, Behzad Kordi. Statistical feature extraction and system identification algorithms for partial discharge signal classification using laguerre polynomial expansion[J]. IEEE Transactions on Dielectrics and Electrical Insulation, 2020, 27(6): 1924-1932.

[17] Xinlu Yang, Wenbo Wang, Ming Fang, Long Hu, Liting Li. Feature Extraction of Partial Discharge Signal Based on Local Mean Decomposition and Multi-scale Singular Spectrum Entropy[J]. Journal of The Institution of Engineers (India): Series B, 2024, 105(2): 265-275.

[18] Salkuti S R. Study on the performance indicators for smart grids: a comprehensive review[J]. TELKOMNIKA (Telecommunication Computing Electronics and Control), 2019, 17(6): 2912-2918.

[19] Banihashemi S, Zhang J. Soft Sensing Image Analysis and Processing Method of Substation Equipment Defects[J]. International Journal for Applied Information Management, 2023, 3(4): 154-161.

[20] Shudong Wang, Yigang He, Baiqiang Yin, Wenbo Zeng, Cong Li, Shuguang Ning. Multi-resolution generalized S-transform denoising for precise localization of partial discharge in substations[J]. IEEE Sensors Journal, 2020, 21(4): 4966-4980.

[21] Jun Jiang, Judong Chen, Jiansheng Li, Xiaoping Yang, Yifan Bie, Prem Ranjan, Chaohai Zhang, Harald Schwarz, et al. Partial discharge detection and diagnosis of transformer bushing based on UHF method[J]. IEEE Sensors Journal, 2021, 21(15): 16798-16806.
[22] Yaseen Ahmed Mohammed Alsumaidaee, Siaw Paw Koh, Chong Tak Yaw, Sieh Kiong Tiong,Chai Phing Chen. Detecting surface discharge faults in switchgear by using hybrid model[J]. Indonesian Journal of Electrical Engineering and Computer Science, 2023, 32(1): 413-422.
[23] Rizvi M. Leveraging Deep Learning Algorithms for Predicting Power Outages and Detecting Faults: A Review[J]. Advances in Research, 2023, 24(5): 80-88.
[24] Bhukya A, Koley C. Bi-long short-term memory networks for radio frequency based arrival time detection of partial discharge signals[J]. IEEE Transactions on Power Delivery, 2021, 37(3): 2024-2031.
[25] Xue J, Wu K, Zhou Y. A risk analysis and prediction model of electric power GIS based on deep learning[J]. International Journal of Computational Science and Engineering, 2019, 18(1): 39-43.
[26] Dukanac D. Extraction of partial discharge signal in predominant VHF range in the presence of strong noise in power transformer[J]. Electrical Engineering, 2023, 105(5): 3001-3018.
[27] Tian D, Chen J, Wang X. Application research of UAV infrared diagnosis technology in intelligent inspection of substations[J]. Energy Informatics, 2024, 7(1): 1-16.
[28] Wu K, Huang X, Yang B, et al. Research on Fault Diagnosis Algorithm of Power Cable Based on Deep Learning[J]. Journal of Electrical Systems, 2024, 20(3): 333-343.
[29] Zhijian Wang, Ningning Yang , Naipeng Li, Wenhua Du, Junyuan Wang. A new fault diagnosis method based on adaptive spectrum mode extraction[J]. Structural Health Monitoring, 2021, 20(6): 3354-3370.
[30] Xin Liu, Hui Liu, Qiang Guo, Caiming Zhang. Adaptive wavelet transform model for time series data prediction[J]. Soft Computing, 2020, 24(8): 5877-5884.
[31] Momeneh S, Nourani V. Forecasting of groundwater level fluctuations using a hybrid of multi-discrete wavelet transforms with artificial intelligence models[J]. Hydrology Research, 2022, 53(6): 914-944.